Bioorg. Med. Chem. 42 (2021) 116245

Contents lists available at ScienceDirect

Bioorganic & Medicinal Chemistry

journal homepage: www.elsevier.com/locate/bmc

Evaluation of carbon-11 labeled 5-(1-methyl-1*H*-pyrazol-4-yl)-*N*-(2-methyl-5-(3-(trifluoromethyl) benzamido)phenyl)nicotinamide as PET tracer for imaging of CSF-1R expression in the brain

Berend van der Wildt [a,b], Madina Nezam [b], Esther J.M. Kooijman [b], Samantha T. Reyes [a], Bin Shen [a], Albert D. Windhorst [b], Frederick T. Chin [a,*]

[a] *Stanford University, School of Medicine, Department of Radiology, Molecular Imaging Program at Stanford (MIPS), 1201 Welch Road, PS049, Stanford, CA 94305-5484, USA*

[b] *Amsterdam UMC, Vrije Universiteit Amsterdam, Radiology & Nuclear Medicine, de Boelelaan 1117, Amsterdam, Netherlands*

ARTICLE INFO

Keywords:
Colony stimulating factor 1 receptor
PET imaging
Carbon-11

ABSTRACT

Pharmacological targeting of tumor associated macrophages and microglia in the tumor microenvironment is a novel therapeutic strategy in the treatment of glioblastoma multiforme. As such, the colony stimulating factor-1 receptor (CSF-1R) has been identified as a druggable target. However, no validated companion diagnostic marker for these therapies exists to date. Towards development of a CSF-1R PET tracer, a set of six compounds based on recently reported CSF-1R inhibitor 5-(1-methyl-1*H*-pyrazol-4-yl)-*N*-(2-methyl-5-(3-(trifluoromethyl)benzamido) phenyl)nicotinamide (Compound **5**) was designed, synthesized and evaluated *in vitro* for potency and selectivity. The highest affinity for CSF-1R was found for compound **5** (IC_{50}: 2.7 nM). Subsequent radiosynthesis of [^{11}C]**5** was achieved in 2.0 ± 0.2% yield (decay corrected to start of synthesis) by carbon-11 carbon monoxide aminocarbonylation in 40 min after end of bombardment. *In vitro* autoradiography with [^{11}C]**5** on rat brain sections demonstrated high specific binding, but also strong off-target binding. *Ex vivo*, only intact tracer was observed in blood plasma at 90 min post injection in healthy rats. PET scanning results demonstrated negligible brain uptake under baseline conditions and this brain uptake did not increase by blocking of efflux transporters using Tariquidar. To conclude, [^{11}C]**5** was successfully synthesized and evaluated in healthy rats. However, the inability of [^{11}C]**5** to cross the blood-brain-barrier excludes its use for imaging of CSF-1R expression in the brain.

1. Introduction

Colony stimulating factor 1 Receptor (CSF-1R or CD115) is a tyrosine kinase that is selectively expressed on microglia in the brain.[1] CSF-1R, which is activated by the endogenous agonists colony stimulating factor and interleukin-34, regulates the survival, proliferation and differentiation of microglia.[2] Outside of the central nervous system CSF-1R is mainly expressed on macrophages. Both microglia and macrophages play a pivotal role in brain diseases involving immune responses such as neuroinflammation, neurodegeneration and glioblastoma.[3] Towards potential treatment these cell types have emerged as targets for therapy. In fact, pharmacological inhibition of CSF-1R, which results depletion of microglia from the brain,[4–6] has shown beneficial effects in various disease models of neuroinflammation and –degeneration and are currently under further investigation in clinical studies.[7]

Positron emission tomography (PET) is an imaging technique that allows for the quantitative imaging of receptor expression in living subjects in a non-invasive manner with good spatiotemporal resolution and high sensitivity. When an appropriate PET tracer is available, PET can be used for selecting patients that would benefit from treatment as well as monitoring disease progression during treatment. As the accumulation of microglia and macrophages at the site of disease in for example glioblastoma will result in a local increase of CSF-1R density, a validated PET tracer for imaging of CSF-1R expression would be of great value in understanding and monitoring CSF-1R targeting therapies. Unfortunately, previously reported CSF-1R PET tracers (Fig. 1) have

* Corresponding author.
E-mail address: chinf@stanford.edu (F.T. Chin).

https://doi.org/10.1016/j.bmc.2021.116245
Received 25 March 2021; Received in revised form 25 May 2021; Accepted 26 May 2021
Available online 30 May 2021

serious shortcomings. [^{18}F]**10** binds to CSF-1R with a low affinity (IC_{50} of 170 nM) and is non-selective with similar affinity for the kinases TrkB and TrkC.[8] Commonly, much lower affinities for receptor binding PET tracers are preferred, in the low to sub-nanomolar range. Another attempt for developing a CSF-1R PET tracer has led to [^{11}C]AZD6495, which in healthy rats and monkeys failed to enter the brain.[9] [^{11}C]CPPC in turn showed good brain uptake in various rodent models of brain disease and non-human primates, however, this tracer suffered from high non-specific binding.[10] Additionally, although no selectivity data on CPPC has been reported, selectivity over other kinases might be minimal as close analogues show high affinity (IC_{50} < 20 nM) for other kinases such as Flt3, Kit, Axl and TrkA.[11–12] [^{11}C]BLZ945, a highly selective CSF-1R inhibitor, was shown to be a substrate for efflux transporters at the blood brain barrier and also suffered from high non-specific binding in the brain.[13] As a result, there still is a clear need for a CSF-1R PET tracer that can overcome the aforementioned limitations.

Recently, a new inhibitor of CSF-1R was reported (5-(1-methyl-1*H*-pyrazol-4-yl)-*N*-(2-methyl-5-(3-(trifluoromethyl)benzamido)phenyl) nicotinamide, compound **5** in Fig. 1).[14] This compound is a potent CSF-1R inhibitor with an IC_{50} of 0.5 nM and a 120-fold selectivity over c-KIT, a closely related kinase family member.[14] Compound **5** has been classified as a type II tyrosine kinase inhibitor, *i.e.* its binding extends from the ATP binding pocket into an adjacent allosteric binding site. As a result, binding was shown to be largely independent on ATP concentration when compared to another CSF-1R inhibitor BLZ945.[14] Given that ATP concentrations in the intracellular environment are high (in the millimolar range) and PET tracer concentrations are extremely low, this non-competitive nature of binding might prove advantageous for *in vivo* PET imaging. Another positive characteristic of this compound are the high metabolic stability in liver microsomes. The PET camera is not able to measure the chemical context of the tracer, but rather detects the annihilation photons that originate from positron emission of the carbon-11 atom, metabolic stability of the PET tracer is important to ensure that the measured signal in the tissue of interest originates from the injected compound. Finally, good cell membrane permeability and a low *in vitro* efflux ratio in a Caco-2 permeability assay (efflux ratio of 2.6 determined as apical to basolateral / basolateral to apical) was considered an important feature. Since the goal of this study was to image CSF-1R expression in the brain, active transport of the PET tracer out of the brain by efflux transporters in the blood brain barrier should be as low as possible. Taken together, compound **5** shows promising characteristics for successful translation into a PET tracer. Therefore, the aim of this study is to translate compound **5**, or a close derivative, into a PET tracer for *in vivo* imaging of CSF-1R expression levels in the brain.

2. Results

2.1. Synthesis and in vitro evaluation

Five analogues of **5** were designed with the goal of identifying a compound that has a high affinity for CSF-1R, a high selectivity towards other kinases and allows for convenient labeling strategies with either carbon-11 or the longer lived ($t_{1/2}$ of 110 min vs 20 min for carbon-11) and thus clinically more relevant isotope fluorine-18. Initially, the position of the nitrogen atom in the pyridine ring was altered from *meta-* to *para-* relative to the carbonyl group, resulting in a structure that is often found as ATP binding pocket motif in kinase inhibitors (*e.g.* BLZ945 Fig. 1, but also sorafenib, regorafenib). Towards obtaining CSF-1R inhibitors that allow for fluorine-18 labelling, the methylpyrazine group on lead compound **5** was selected for substitution with a fluoroethylpyrazine or a fluoroethyltriazole group. The methylpyrazine group was chosen for modification as this moiety appears to allow for modification without negatively effecting the affinity.[14] Also, a methylamide group was introduced as a substitute for methylpyrazine. A methylamide substitute as in **BLZ945** was selected as this would lower molecular weight as well as polar surface area and thus would increase the blood brain barrier penetration.

The chemistry towards the target molecules is depicted in Scheme 1. First, methyl nitroaniline was reacted with trifluoromethylbenzoyl chloride to obtain nitrophenyl derivative **1**. Béchamp reduction resulted in aniline derivative **2**, which was esterified with either bromonicotinoyl or bromoisonicotinoyl chloride to afford aryl bromides **3** and **4**. These arylbromides were subjected to a Suzuki cross-coupling reaction with methylpyrazole boronic acid pinacol ester to obtain compounds **5** and **6**.[15] When evaluating the CSF-1R inhibitory potential of these compounds it became clear that the nitrogen atom is preferably located at the *meta* position (Table 1, entry 3, compound **5**) as placing the nitrogen at the *para* position results in a decrease in affinity by a factor of 10 (Table 1, entry 2, compound **4**). Importantly, the IC_{50} value of 2.7 ± 0.4 nM for compound **5** corresponds fairly well with the previously reported value of 0.5 nM.[14] The small difference appears to be inherent to the

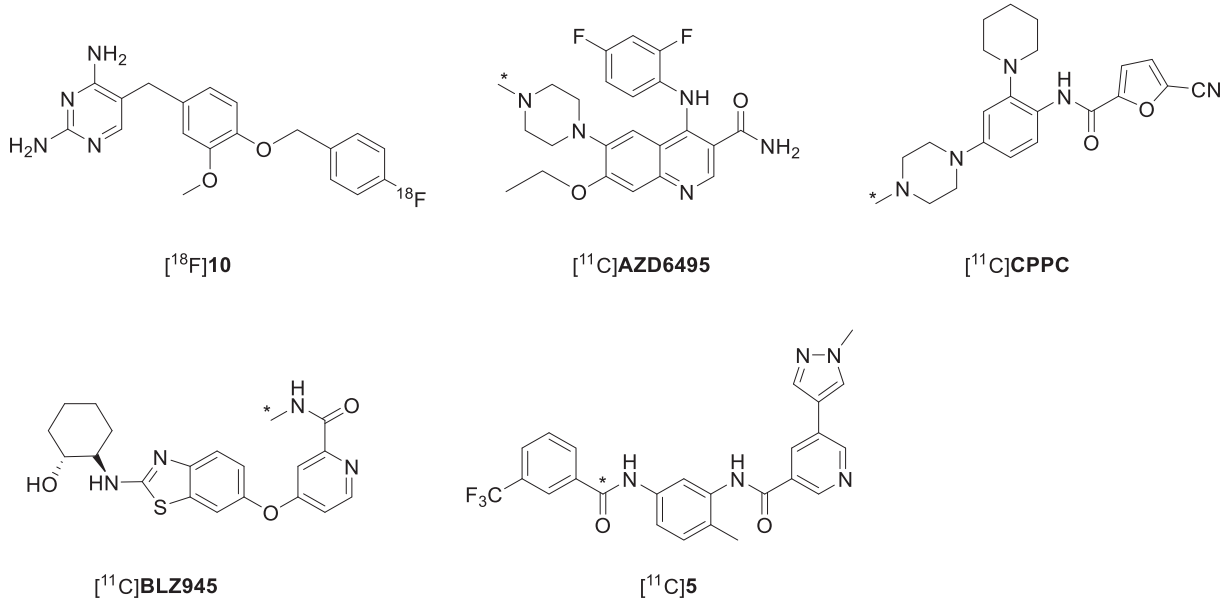

Fig. 1. CSF-1R PET tracers previously developed[8–10,13] and [^{11}C]**5** (this work). The position of the carbon-11 labels are depicted with *.

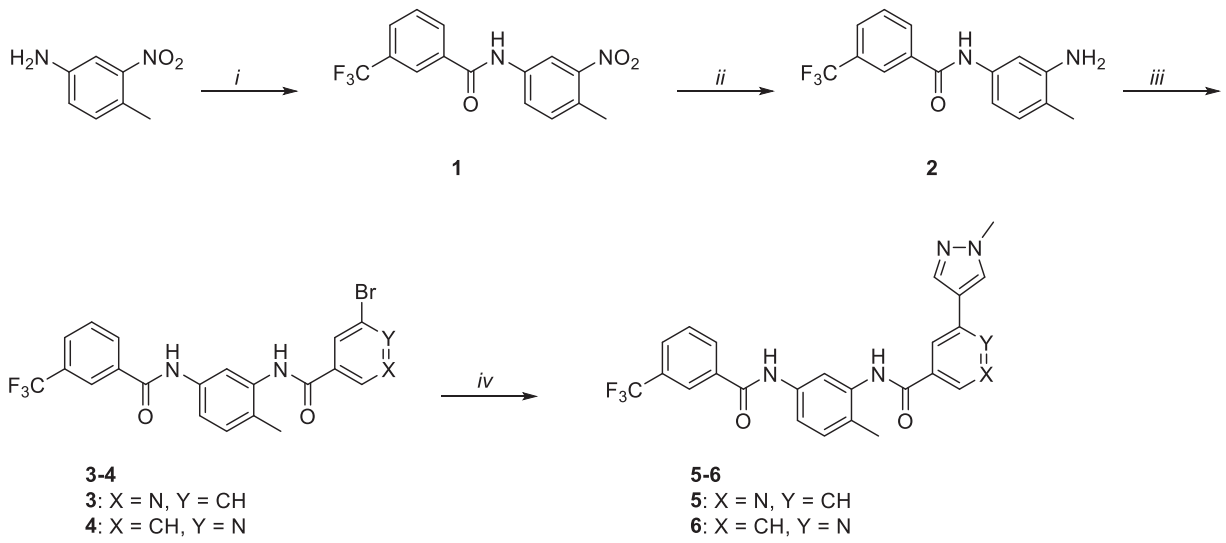

Scheme 1. Synthesis of compound **5** and its closely related analogue **6**. Reagents and conditions: *i*) 3-(trifluoromethyl)benzoyl chloride, TEA, DCM, 3 h, rt, 97%; *ii*) HCl, Fe, H_2O/EtOH, 4 h, reflux, 94%; *iii*) First, appropriate bromopyridine carboxylic acid, oxalyl chloride, THF/DCM/DMF, 2 h, rt, then compound **2**, TEA, DCM, 16 h, rt, 79–88%; *iv*) 1-methylpyrazole-4-boronic acid pinacol ester, $Pd(PPh_3)_4$, CsF, MeOH/DMF, 16 h, 70 °C, 68–88%.

Table 1
IC_{50} values for tested compound for CSF-1R, PDGFR-β and c-KIT.

Entry	Compound	IC_{50} (nM)			Ratio	
		CSF-1R	PDGFR-β	c-KIT	CSF-1R/PDGFR-β	CSF-1R/c-KIT
1	BLZ945	6.9 ± 0.5	>1000	>1000		
2	**4**	30.6 ± 7.2	n.d.	n.d.		
3	**5**	2.7 ± 0.4	6.3 ± 1.2	4.5 ± 1.0	2.31	1.64
4	**8**	40.0 ± 3.1	2.5 ± 0.9	3.8 ± 2.3	0.06	0.09
5	**9**	29.5 ± 3.6	45.6 ± 2.3	27.4 ± 3.7	1.55	0.93
6	**12**	21.7 ± 1.5	27.8 ± 5.0	1.0 ± 3.5	1.28	0.04
7	**20**	77.2 ± 5.9	n.d.	n.d.		

Values are expressed as the average ± standard deviation of at least 3 experiments.
n.d.: not determined.

used assay as BLZ945 gave an IC_{50} value of 6.9 nM in our assay compared to a reported value of 1.0 nM.[4]

Subsequently, modifications were made to the methylpyrazole group (Scheme 2). A Suzuki reaction[15] with between fluoroethylpyrazole boronic acid pinacol ester **7** and compound **3** gave fluoroethyl analogue **8**. Methylamide analogue **9** was obtained by a 2-step palladium catalyzed carbonylation reaction using trichlorophenyl formate.[16] A Sonogashira reaction[17] between arylbromide **3** and trimethylsilylacetylene resulted in TMS- protected alkyne **10**, which after deprotection, was reacted with fluoroethylazide in a copper catalyzed 1,3-dipolar cycloaddition ('Click' reaction[18]) to obtain triazole **12**.

Substitution of methyl for fluoroethyl on the pyrazole group (compound **8**) was not well tolerated and resulted in an IC_{50} of 40 nM. Methylamide instead of methylpyrazole (compound **9**), a similar structural motif as used in the well-known CSF-1R inhibitor BLZ945, still retained a fair affinity but did not result in an improvement (IC_{50}: 30 nM). Fluoroethyltriazole group as substitute for methylpyrazole (compound **12**) resulted in a modest decrease with an IC_{50} of 22 nM. Overall, analogues that allow for fluorine-18 labeling have been identified, although no compounds with higher potency than compound **5** (IC_{50}: 2.7 ± 0.4 nM) were discovered.

Next, selectivity towards c-Kit and PDGFR-β, kinases with strong structural homology to CSF-1R, was evaluated. To our surprise, **5** showed only a slight selectivity towards CSF-1R by a factor of 2 over both c-KIT and PDGFR-β, unlike the 120-fold selectivity over c-Kit that was previously reported.[14] Fluoroethyl analogue **8** showed a lower selectivity, with IC_{50} values for PDGFR-β and c-KIT of approximately 4 nM, lower than observed for CSF-1R. Similar results were obtained for the triazole analogue **12**. A good selectivity for CSF-1R over PDGFR-β was found for compound **9** (10-fold), however, not over c-KIT (0.5-fold). Overall, the more bulky fluoroethyl group at the pyrazole ring resulted in lower affinities and the optimal position for the nitrogen atom in the pyridine ring is on the original *meta*-position. Unfortunately, no selectivity for CSF-1R was observed for any of the compounds.

In previous medicinal chemistry efforts towards compound **5**, a methylpiperazine group on the trifluoromethylbenzene ring had been removed from the structure due to metabolic instability in mouse liver microsomes, however, at the cost of a 400-fold decrease in affinity for CSF-1R and a 2000-fold decrease in selectivity over c-KIT.[14] Reintroduction of this functionality, which is quite a general motif in approved drugs (like imatinib, masitinib among other kinase inhibitors), could result in an increase in affinity as well as in selectivity. The convergent synthesis towards compound **20** is depicted in Scheme 3.

Methyltrifluorobenzoic acid was methylated and subsequently brominated with NBS in a radical reaction to afford bromomethyl benzoate **14**. A nucleophilic substitution using methylpiperazine followed by saponification resulted in carboxylic acid **16**. EDC mediated condensation of nitromethylaniline and 5-bromonicotinic acid afforded aryl bromide **17**, which was subject to a Suzuki reaction with methylpyrazoleboronic pinacol ester to afford methylpyrazole **18**. Béchamps reduction and subsequent condensation with **16** resulted in **20** as a potential CSF-1R inhibitor with high affinity and selectivity. Subsequent testing for potency was, however, disappointing with an IC_{50} value for CSF-1R of only 77 nM. Therefore, no further testing of this compound for selectivity was performed.

2.2. Radiochemistry

The most promising compound in this series, compound **5**, was selected for radiolabeling and further evaluation *in vivo*. A palladium

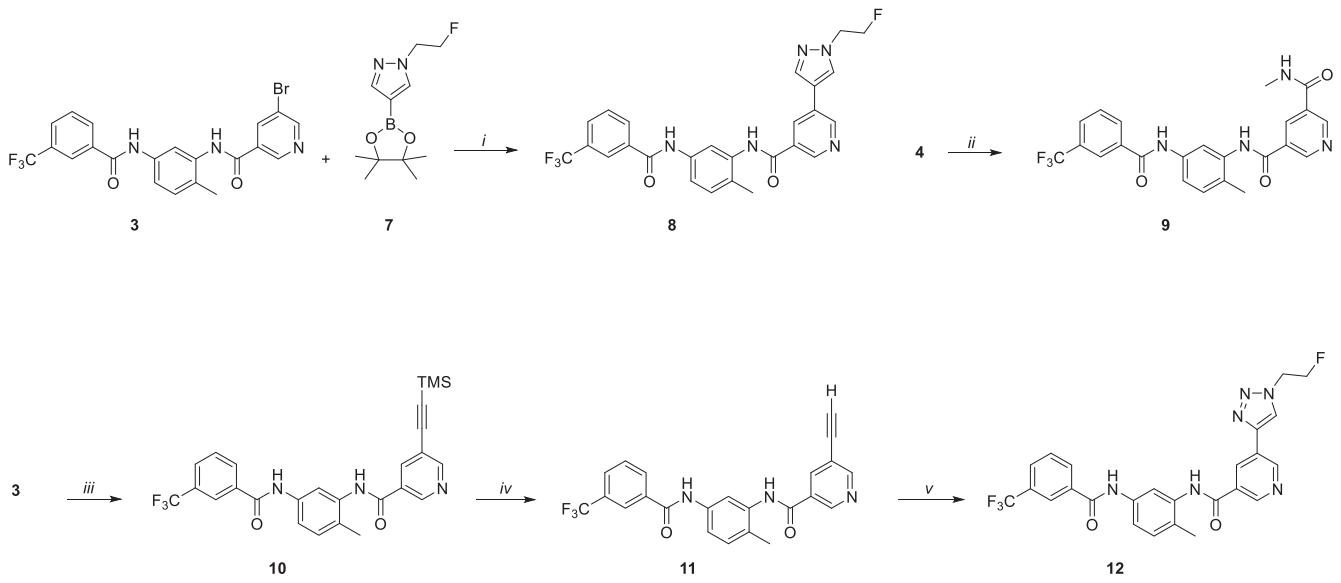

Scheme 2. Synthesis of analogues of compound **5**. Reagents and conditions: *i*) Compound **3** and **7**, $Pd(PPh_3)_4$, CsF, MeOH/THF, 16 h, reflux, 73%; *ii*) First, compound **4**, 2,4,6-trichlorophenyl formate, $Pd(OAc)_2$, xantphos, NaOAc, dioxane, 80 °C, 16 h. Then, methylamine·HCl, TEA, DMF, 3 h, rt, 35%; *iii*) trimethylsilylacetylene, $PdCl_2(PPh_3)_2$, CuI, TEA, DMF, rt, 16 h, 71%; *iv*) CsF, THF, rt, 16 h, 99%; *v*) 2-azido-1-fluoroethane, $CuSO_4{\cdot}5H_2O$, Na-ascorbate, DMF/H_2O, 80 °C microwave irradiation, 10 min, 55%.

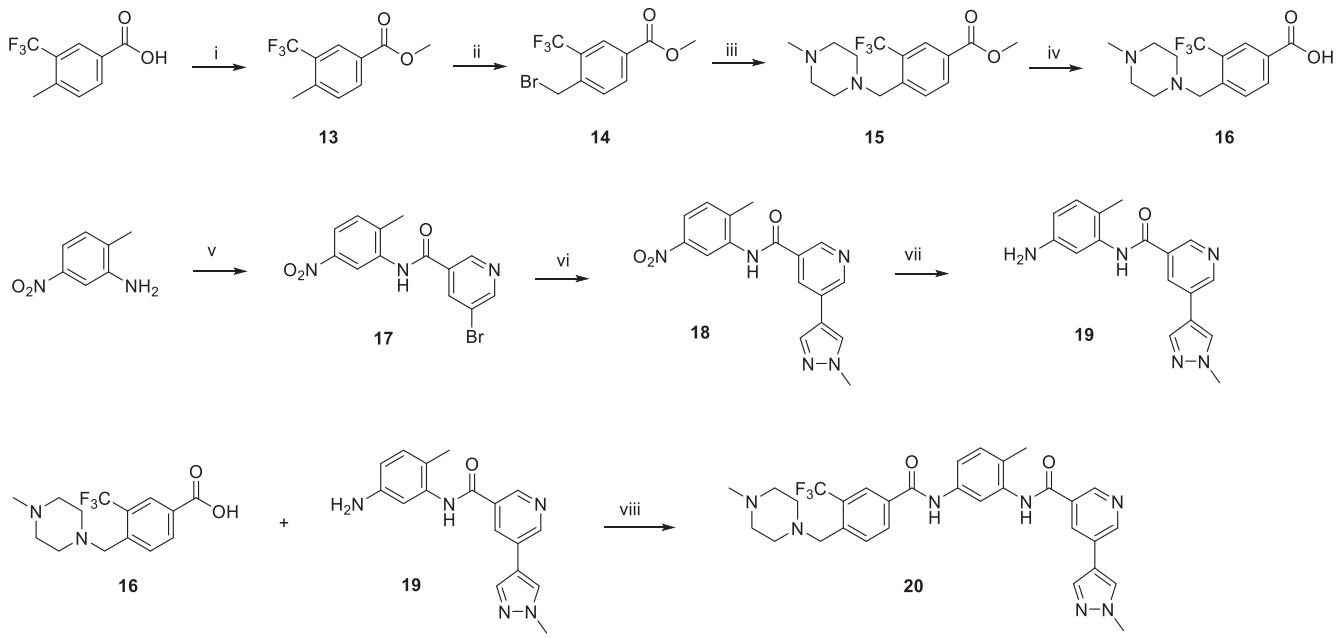

Scheme 3. Synthesis of methyl piperazine analogue **20**. Reagents and conditions: *i*) CH_3I, K_2CO_3, DMF, 16 h, rt, 87%; *ii*) *N*-bromosuccinimide, benzoyl peroxide, MeCN, 16 h, reflux, 74%; *iii*) 1-methylpiperazine, K_2CO_3, MeCN, 16 h, reflux, 63%; *iv*) NaOH, H_2O/EtOH, 6 h, rt, 46%; *v*) 5-bromonicotinic acid, EDC, DMAP, DMF, 16 h, rt, 59%; *vi*) 1-methylpyrazole-4-boronic acid pinacol ester, $Pd(PPh_3)_4$, CsF, DMF, 16 h, 100 °C, 59%; *vii*) NH_4Cl, Fe, H_2O/EtOH, 2 h, 70 °C, 90%; *viii*) EDC, DMAP, DMF, 16 h, rt, 71%.

mediated carbon-11 carbon monoxide aminocarbonylation reaction was chosen as depicted in Table 2. This reaction is supposed to result in [^{11}C]**5**, an isotopologue of **5** that will behave similarly with the exception of positron emission of the carbon-11 atom. Conveniently, precursor **19** was already available as it was used as intermediate in the synthesis of compound **20**.

To efficiently screen various reaction conditions, we used a low pressure semi-automated [^{11}C]CO dispensing system using xenon as a carrier gas.[19,20] Xantphos as preferred ligand is carbonylation reactions[21] was used throughout the screening. Initially, the reaction was executed in the absence of a base (Table 2, entry 1). Using these conditions no product was observed, in parallel with previous reports of aminocarbonylations on aniline derivatives.[22,23] Also, using *N,N*-diisopropylethylamine (DIPEA) as a weak base did not result in any [^{11}C]**5** (entry 2. Li-HMDS, a strong base, did result in the conversion of [^{11}C]CO to non-volatile compounds (entry 3, 98% trapping efficiency), however again no product was obtained. Success was achieved using 1,8-diazabicyclo(5.4.0)undec-7-ene (DBU), which resulted in a good radiochemical yield of 31 ± 8% (Entry 4). Variation in the palladium source (entry 5, 6) resulted in lower yields. Finally, different amounts of amine precursor **19** (entry 7–10) did not result in increased radiochemical yields when compared to the conditions depicted in entry 4.

Table 2

Optimization of radiolabeling conditions towards [^{11}C]**5**.

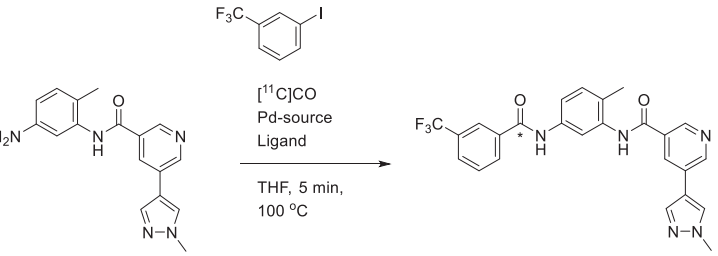

Entry	Amine (μmol)	Base	Catalyst	Trapping efficiency (%)	Radiochemical purity (%)	Radiochemical yield (%)	n
1	10	–	$PdCl_2(PPh_3)_2$	37	0	0	1
2	10	DiPEA	$PdCl_2(PPh_3)_2$	15	0	0	1
3	10	Li-HMDS	$PdCl_2(PPh_3)_2$	98	0	0	1
4	10	DBU	$PdCl_2(PPh_3)_2$	85 ± 14	37 ± 8	31 ± 8	5
5	10	DBU	Pd_2dba_3	84 ± 0	5 ± 1	4 ± 0	3
6	10	DBU	$Pd_2[\pi\text{-}cinnamyl]Cl_2$	87 ± 6	21 ± 1	18 ± 2	3
7	0	DBU	$PdCl_2(PPh_3)_2$	82 ± 9	0 ± 0	0 ± 0	3
8	2.5	DBU	$PdCl_2(PPh_3)_2$	73 ± 2	24 ± 4	17 ± 3	3
9	5	DBU	$PdCl_2(PPh_3)_2$	77 ± 5	29 ± 7	22 ± 4	3
10	20	DBU	$PdCl_2(PPh_3)_2$	78 ± 5	17 ± 0	14 ± 1	3

General method: Reactions were performed with trifluoro-iodobenzene (2.7 mg, 10 μmol), base (20 μmol), xantphos (2.9 mg, 5 μmol) and palladium (2 μmol) in THF (0.7 mL). Reactions mixtures were heated at 100 °C for 5 min. The results are expressed as average trapping efficiency (percentage of non-volatile radioactive products after reaction), radiochemical purity (percentage of radioactive product area under the curve (AUC) relative to the total AUC), and radiochemical yield (the product of trapping efficiency and radiochemical purity) (number of experiments 'n' is depicted in the last column).

The conditions depicted in entry 4 were considered optimal and were thus used for full scale synthesis of [^{11}C]**5**. After preparative HPLC and solid phase extraction reformulation, [^{11}C]**5** was obtained in 2.0 ± 0.2% decay corrected yield based on the starting amount of [^{11}C]CO_2 (109 ± 25 MBq in 2 mL of 10% ethanol in saline, n = 3) in 40 min using a semi-automated synthesis procedure. The product identity was confirmed by co-injection of an authentic reference standard of compound **5**. No chemical contaminations were observed and radiochemical purity was > 99% (see supporting information Fig. 4 for chromatograms). Molar activity was determined as 181 ± 22 GBq·μmol^{-1}. The formulated product retained a radiochemical purity of > 95% up to 1 h after end of synthesis.

2.3. *In vitro, ex vivo and in vivo evaluation*

The partition coefficient logD of the compound was determined by shake-flask method to be 2.54 ± 0.02, well within the range for brain penetration by passive diffusion.

In vitro binding experiments on healthy rat brain sections using autoradiography were performed. Due to the widespread presence of microglia in the brain, which express CSF-1R, a homogeneous expression pattern would be expected. Indeed, [^{11}C]**5** shows high binding throughout the rat brain (Fig. 2A). However, binding was not as homogeneous as expected, with hippocampus and cortex showing strong binding at baseline conditions. The total binding could be largely blocked by co-incubation with excess unlabeled **5** (Fig. 2). Despite this high specific binding, selective binding to CSF-1R seemed marginal, as co-incubation with excess **BLZ945**, a highly selective CSF-1R inhibitor, only decreased the binding of [^{11}C]**5** by approximately 20%. This incomplete blocking of [^{11}C]**5** binding could very well be attributed to the low selectivity of compound **5** when compared to other kinases such as c-KIT and PDGFR-β. Blocking with the broad spectrum kinase inhibitor CPPC [11, 12] resulted in a more profound reduction in [^{11}C]**5** binding of approximately 50%.

PET imaging in healthy rats showed poor brain uptake of [^{11}C]**5** throughout the entire scan (Fig. 3A and B). After an initial peak directly after tracer injection, which is the result of perfusion, activity concentrations remain extremely low (Fig. 3B). Blocking of efflux transporters did not significantly increase the brain concentrations of [^{11}C]**5**, which excludes that strong efflux is causing the low brain uptake levels.

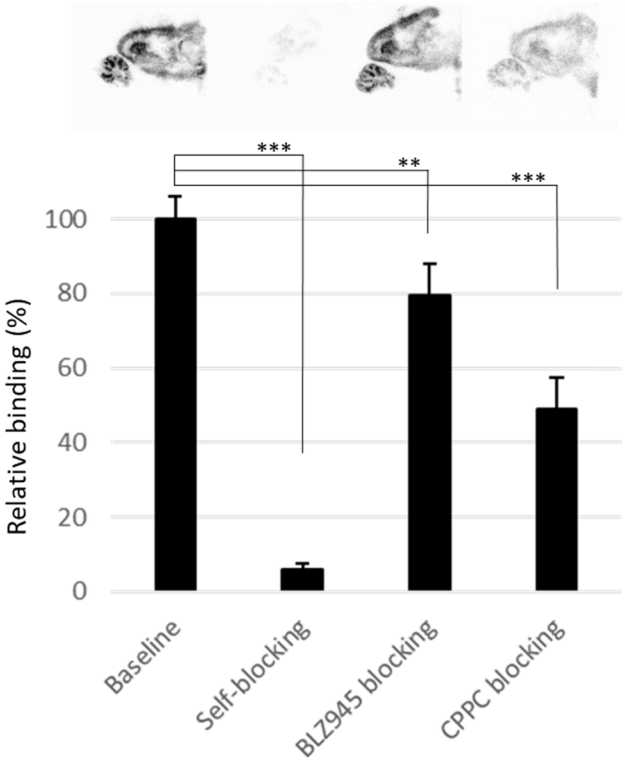

Fig. 2. *In vitro* autoradiography on rat brain using [^{11}C]**5**. Representative images of brain sections are shown at baseline, self-blocking conditions, BLZ945 and CPPC blocking. CSF-1R inhibitors were used at 10 μM concentration. The results are expressed as average normalized binding ± standard deviation (n = 3).

Metabolism of [^{11}C]**5** into polar, non-brain permeable radioactive compounds was not observed either and thus can be excluded as an explanation for low brain uptake. In fact, only parent radiotracer was detected in the blood plasma at 90 min post injection (Supporting information Fig. 5). Corresponding to the lack of brain uptake, no

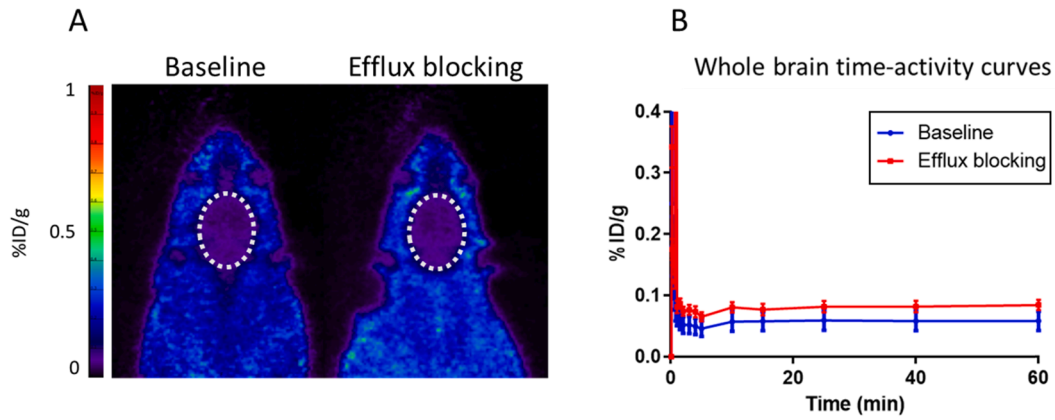

Fig. 3. In vivo PET imaging in healthy rats. 3A: representative summed PET images of rats (cross-section, axial view) injected with [^{11}C]**5** at baseline (Left) or efflux transporter blocking conditions (Right, tariquidar, 15 mg·kg^{-1}, i.v. administration 30 min prior to tracer injection). The location of the brain is indicated with dotted oval shapes in gray. Other colors depict the radioactivity concentrations in %ID/g according to the scale bar. 3B: Whole brain time-activity curves following injection of [^{11}C]**5** under baseline of efflux transporter blocking conditions. Results are expressed as average ± standard deviation (n = 2 per group).

radioactive compounds could be extracted from the brain for radiometabolite analysis.

3. Discussion

Compound **5** was selected for this study due to its very high affinity for CSF-1R and its reported 120-fold selectivity over c-KIT, a close CSF-1R homologue.[14] In addition, binding of this compound to CSF-1R was, in contrast to many kinase inhibitors, non-competitive with ATP. This could theoretically result in improved imaging characteristics as binding *in vivo* is not hampered by ATP, which is present at high concentrations in the intracellular environment. In our hands, however, the selectivity of compound **5** for CSF-1R was very minimal and in fact the compound was found to be equipotent for both other kinases evaluated, c-KIT and PDGFR-β. The discrepancy between the reported and determined values is unclear. However, this non-selective behavior might not come as a complete surprise though, as the structure of compound **5** shows structural overlap with the tyrosine kinase inhibitor imatinib and masitinib, which both target c-KIT, PDGFR-β and, to a lesser extent, CSF-1R. It must be noted that both c-KIT and PDGFR-β have been identified as drug targets in cancer treatment and are pursued for PET and SPECT tracer development as well.[24–27] Therefore, the non-selective PET tracer [^{11}C]**5** might very well be useful as predictive tool for identification of cancer patients who respond to broad spectrum kinase inhibitor therapy.[28]

In our efforts to finding compounds with increased affinity for CSF-1R or improved selectivity over other kinases no better compounds than lead compound **5** were identified. However, a moderately c-KIT selective inhibitor was identified (compound **12**) that allows for fluorine-18 labeling and could potentially be used for peripheral c-KIT imaging.

Three obvious positions for carbon-11 labeling can be identified in the structure of compound **5**. Methylation using [^{11}C]methyl iodide or [^{11}C]methyl triflate at the pyrazole group could be performed in the presence of a strong base.[29] However, such strong basic conditions could easily result in alkylation of either of the two amide groups as well. A more selective reaction would be palladium mediated [^{11}C]CO aminocarbonylation between an aniline derivative and aryl halide. Both amides are theoretically accessible for labeling, however the current approach was chosen due to the commercial availability of 1-iodo-3-trifluoromethylbenzene. The carbon-11 label might also be inserted at this position by employing carbon-11 trifluoromethylbenzoyl chloride as radioactive precursor. This radiochemistry would proceed in a multistep fashion where at first cyclotron produced [^{11}C]CO_2 is reacted with a Grignard reagent to obtain carbon-11 trifluoromethylbenzoic acid, which after conversion to the corresponding acyl chloride can react with the amine precursor **19** to form [^{11}C]**5.**[30] Clearly, this multistep procedure with several purification steps is not preferred when working with the short-lived isotope carbon-11. Exploring the proposed [^{11}C]CO carbonylation chemistry, it was found that in the absence of a base or using a mild base (DiPEA) no product was formed and mainly unreacted [^{11}C]CO was found, in correspondence with earlier reports on aminocarbonylations on aniline derivatives.[22,23] Using Li-HMDS resulted in the formation of many side products. The formation of [^{11}C]**5** was only observed when DBU was used as a base. Together with $PdCl_2(PPh_3)_2$ as a preferred catalyst, these conditions were reported to provide optimal results in [^{11}C]CO carbonylation reactions before.[31] The overall isolated yield was fairly low (2.0 ± 0.2% d.c. based on [^{11}C]CO_2,) compared to the results obtained during test screening reactions (31 ± 8% based on [^{11}C]CO). This difference can be partially explained by the fact that the isolated yield is based on [^{11}C]CO_2, whereas during the optimization reactions the yield was calculated based on [^{11}C]CO. Molybdenum, although reliable and long-lasting as catalyst, does not convert CO_2 to CO as efficiently as zinc does.[32] Additionally, a fairly large loss of [^{11}C]CO was observed at the full scale experiments when retracting the [^{11}C]CO-inlet needle from the reaction vial after [^{11}C]CO transfer. This effect was not obviously seen or perhaps overlooked when dispensing [^{11}C]CO over several vials manually. Finally, at large scale radiosynthesis the trapping efficiencies dropped significantly. This is potentially due to the larger amount of xenon carrier gas in a single vial, although no further experiments were conducted to confirm this hypothesis. Overall, [^{11}C]**5** could be obtained in excellent chemical and radiochemical purity in sufficient amounts and radioactivity concentrations for our studies (supporting information Fig. 4). For future studies, or studies performed in PET centers that do not readily have access to [^{11}C]CO, it could be interesting to explore labeling of compound **5** with the longer lived isotope fluorine-18 by means of fluorine-18 trifluoromethylation.[33]

In vitro autoradiography showed very high specific binding on rat brain sections, as demonstrated by the 95% reduction in [^{11}C]**5** binding when co-incubating with excess unlabeled **5**. Selective binding to CSF-1R, however, appears limited as evidenced by a 20% reduction in binding when co-incubating with unlabeled BLZ945, a highly selective CSF-1R inhibitor.[4] The residual tracer binding might be attributed to binding to other targets such as c-KIT and PDGFR-β, both not blocked by BLZ945. Blocking with CPPC resulted in a stronger reduction of [^{11}C]**5** binding of about 50%. CPPC has previously been claimed to be a selective CSF-1R inhibitor.[8] Although no selectivity data of CPPC is available in literature, structurally close analogs are broad spectrum kinase inhibitors, displaying IC_{50} values below 0.1 μM for FLT3, c-KIT, AXL, TRKA, and LCK.[11,12] However, even CPPC did not provide the same

blocking effect as when coincubating with unlabeled compound **5** (self-blocking). Therefore, it is likely that [^{11}C]**5** binds to more kinases or other biological targets than tested in this work. To elucidate the selectivity profile of compound **5**, a full spectrum kinase screening should be performed.

PET imaging results unfortunately showed no brain uptake for [^{11}C]**5** at any given time-point. Blocking of efflux transporters using tariquidar had no effect on brain uptake, despite blocking at a dose of 15 mg/kg that blocks the main efflux transporters P-GP and BCRP.[34,35] A blood plasma metabolite analysis excluded the possibility that rapid metabolism of [^{11}C]**5** into more polar and thus brain-impermeable radiometabolites was the cause of this low brain uptake. In fact, only intact tracer was observed in blood plasma after 90 min post injection (supporting information Fig. 5). The reason for the low brain uptake must therefore be attributed to the physiochemical properties of compound **5**. A good measure for scoring compounds for successful PET imaging is PET-CNS-MPO,[36] a CNS PET tracer scoring tool derived from CNS-MPO.[37] Although the CNS-MPO score of compound **5** of 3.3 is close to the desired value of > 4, the score of 1.3 in the CNS-MPO-PET method is far below the desired score of > 3 (supporting information Table 1).

Overall, the current work has identified compound **5** as a broad spectrum inhibitor, despite earlier reports on selectivity. A radiolabeling procedure was developed to obtain [^{11}C]**5** in sufficient radiochemical yields for further studies. *In vitro* binding of [^{11}C]**5** appears highly selective, although at this point the selectivity profile is unknown and this should likely be elucidated prior to performing additional imaging studies, *e.g.* peripheral tumor imaging studies. The clear lack of brain uptake excludes this radiotracer from imaging of CSF-1R or other kinases in the brain.

4. Conclusion

[^{11}C]**5** was successfully synthesized and evaluated in healthy rats. The inability of [^{11}C]**5** to cross the blood–brain-barrier in rats, however, excludes its use for imaging of CSF-1R expression in the brain. Compound [^{11}C]**5** could be useful for *in vivo* imaging of kinase expression in tumors in the periphery, although at first a thorough kinase selectivity study seems warranted. Future work towards identifying a PET tracer for imaging of CSF-1R expression in the brain will be focusing on structurally distinct CSF-1R inhibitors.

5. Materials and methods

5.1. General

All chemical reagents and solvents were obtained from commercial suppliers and used as received. Microwave reactions were performed on a CEM Discover Legacy (Matthews, NC, USA). Reaction monitoring was performed by thin layer chromatography on pre-coated silica 60 F254 aluminium plates (Merck, Darmstadt, Germany). Spots were visualized with UV light (254 nm), KMnO4 or ninhydrin staining. NMR spectroscopy was performed using an Agilent 400 MR (Agilent Technologies, Santa Clara, CA, USA) with chemical shifts (δ) reported in parts per million (ppm) relative to the solvent ($CDCl_3$ 1H: 7.26 ppm, ^{13}C: 77.16 ppm; DMSO-d_6 1H: 2.50 ppm, ^{13}C 39.52 ppm; CD_3OD ^{1}H: 3.31 ppm, ^{13}C: 49.00 ppm). High resolution mass spectrometry was performed on a Bruker Daltonics - apex-Qe (Bruker, Billerica, MA, USA) in either positive or negative ion mode. Enzyme inhibition assay kits (Z-LYTETM assay) and human recombinant enzymes were from ThermoFisher Scientific (Waltham, MA, USA). Fluorescent readout of 384-well plates was performed on a fluorimeter (Safire, Tecan, XFluo). Carbon-11 was prepared by the ^{14}N(p,α)^{11}C nuclear reaction using a mixture of 0.5% O_2/N_2 as target gas on an IBA Cyclone 18/9 cyclotron (IBA, Louvain-la-Neuve, Belgium) and was delivered as [^{11}C]CO_2 to the experimental set up using helium as a carrier gas. Analytical HPLC was performed on a Jasco (Easton, MD, USA) PU-2089 pump station equipped with a Grace Platinum column (5 μm, 250 mm × 4.6 mm using H_2O/MeCN/TFA (60:40:0.1; v/v/v) as a mobile phase at a flow rate of 1 mL·min^{-1}, with a Jasco UV-2075 UV detector ($\lambda = 254$ nm) and a NaI radioactivity detector (Raytest, Straubenhardt, Germany). Chromatograms were acquired with Raytest GINA Star software (version 5.01). Preparative HPLC for isolation of the radiotracer was performed on a Jasco PU-2089 pump station equipped with a Phenomenex Luna C18 column (10 μm, 250 mm × 10 mm) using H_2O/MeCN/TFA (45:55:01; v/v) as eluent at a flow rate of 5 mL·min^{-1}, a Jasco UV-1575 Plus UV detector ($\lambda = 254$ nm), a custom made radioactivity detector and Jasco ChromNAV CFR software (version 1.14.01) for data acquisition. Wistar Rats (RccHan Wist, male, 8–10 weeks, approximately 250 g) were obtained from Envigo and were housed under standard conditions (24 °C, 60% relative humidity, 12 h light/dark cycles) and provided with water and food *ad libitum*. Tariquidar was freshly formulated as 3.75 mg/mL tariquidar in 2.5% (g/v) aqueous dextrose solution prior to iv administration. RadioTLC plates were exposed to a phosphorimager screen ((GE Healthcare) for 30 min in a cassette (Hypercasette, Amersham Biosciences, Little Chalfont, United Kingdom) and subsequently developed using a Typhoon Trio Imager (GE Healthcare). Images were analyzed using ImageQuant TL (GE Healthcare). Dynamic PET imaging was performed using dedicated small animal NanoPET/CT and NanoPET/MR scanners (Mediso Ltd., Hungary, Budapest) with identical PET components. PET scans were acquired in list mode and rebinned into the following frame sequence: 4 × 5, 4 × 10, 2 × 30, 3 × 60, 2 × 300, 1 × 600, 1 × 900 and 1 × 1200 s. Reconstruction was performed with a fully 3-dimensional (3D) reconstruction algorithm using four iterations and six subsets, resulting in an isotropic 0.4-mm voxel dimension. Images were analyzed using VivoQuant™ (Invicro, Boston, MA, USA) by drawing a region of interest over the full brain.

5.1.1. (N-(4-methyl-3-nitrophenyl)-3-(trifluoromethyl)benzamide)

To a solution of 4-methyl-3-nitroaniline (5.04 g, 33.1 mmol) and TEA (5.00 g, 49.5 mmol) in DCM (30 mL) was added 3-(trifluoromethyl) benzoyl chloride (6.90 g, 33.1 mmol) dropwise. After stirring for 3 h at rt, the solution was diluted with 1 M HCl (30 mL). The solids were filtered, washed with water and DCM and dried to obtain the title compound as a white solid (10.4 g, 97%). ^{1}H NMR (400 MHz, DMSO-d_6): $\delta = 10.77$ (s, 1H), 8.52 (d, 1H, $J = 2.3$ Hz, 8.32 (s, 1H), 8.27 (d, 1H, $J = 7.9$ Hz), 7.99 (m, 2H), 7.80 (t, 1H, $J = 7.8$ Hz), 7.50 (d, 1H, $J = 8.9$ Hz), 2.50 (s, 3H, overlaps with DMSO signal); ^{13}C NMR (101 MHz, DMSO-d_6): $\delta = 164.3$, 148.5, 137.7, 135.1, 133.1, 131.9, 129.8, 129.2 (d, $J = 32.1$ Hz), 128.5 (d, $J = 3.5$ Hz), 128.0, 125.0, 124.3 (d, $J = 3.5$ Hz), 123.4 (d, $J = 272.6$ Hz), 115.7, 19.3; ESI-HRMS: *m/z* calculated for $C_{15}H_{11}F_3N_2NaO_3$: 347.0619; found: 347.0615 $[M + Na]^+$.

5.1.2. (N-(3-amino-4-methylphenyl)-3-(trifluoromethyl)benzamide)

To a solution of compound **1** (6.00 g, 18.5 mmol) in ethanol/H_2O (4:1, 30 mL) was added 1 mL conc. HCl and iron powder (5.16 g, 92.5 mmol). The mixture was refluxed for 4 h followed by filtration over Celite. After concentration, the mixture was partitioned between DCM (50 mL) and sat. $NaHCO_3$ (50 mL). The organic layer was washed with $NaHCO_3$ (2 × 50 mL) and brine (50 mL). After drying on Na_2SO_4, filtration and concentration, the product was obtained as a white solid (5.30 g, 97%).^{1}H NMR (400 MHz, DMSO-d_6): $\delta = 10.14$ (s, 1H), 8.24 (m, 2H), 7.93 (d, 1H, $J = 7.8$ Hz), 7.77 (t, 1H, $J = 7.8$ Hz), 7.11 (s, 1H), 6.84 (m, 2H), 4.88 (s, 2H), 2.03 (s, 3H); ^{13}C NMR (101 MHz, DMSO-d_6): $\delta = 163.5$, 146.6, 137.2, 136.1, 131.7, 129.7, 129.6, 129.1, 127.8 (d, $J = 3.6$ Hz), 124.1 (d, $J = 3.9$ Hz), 124.0 (d, $J = 272.6$ Hz), 117.2, 108.8, 106.5, 17.0; ESI-HRMS: *m/z* calculated for $C_{15}H_{14}F_3N_2O$: 295.1053; found 295.1055 $[M + H]^+$.

5.1.3. (5-bromo-N-(2-methyl-5-(3-(trifluoromethyl)benzamido)phenyl) nicotinamide)

To a solution of 5-bromonicotinic acid (1.1 g, 5.5 mmol) in THF (5 mL) and DCM (5 mL) and DMF (0.2 mL) was added oxalic chloride (0.47

mL, 5.5 mmol). The resulting solution was stirred for 2 h at rt. After concentration in vacuo, the residue was taken up in DCM (10 mL) and a solution of compound **2** (1.5 g, 5.0 mmol) and TEA (1.5 mL, 11 mmol) in DCM (10 mL) was added. The resulting mixture was stirred overnight and diluted with DCM (50 mL) and 1 M HCl (50 mL). The solids were collected by filtration, rinsed with water and DCM to obtain the product as a white solid (2.1 g, 88%). ^{1}H NMR (400 MHz, DMSO-d_6): δ = 10.51 (s, 1H), 10.24 (s, 1H), 9.13 (s, 1H), 8.92 (s, 1H), 8.57 (s, 1H), 8.32 (s, 1H), 8.28 (d, 1H, J = 7.9 Hz), 7.95 (d, 1H, J = 7.8 Hz), 7.90 (s, 1H), 7.78 (t, 1H, J = 7.8 Hz), 7.63 (d, 1H, J = 8.3 Hz), 7.28 (d, 1H, J = 8.4 Hz), 2.25 (s, 3H). ^{13}C NMR (101 MHz, DMSO-d_6): δ = 163.9, 162.5, 152.8, 147.3, 137.8, 136.9, 135.7, 135.7, 131.8, 131.7, 130.4, 129.7, 129.3, 129.2 (q, J = 32.1 Hz), 128.1 (q, J = 3.6 Hz), 124.2 (q, J = 3.9 Hz), 124.0 (q, J = 272.4 Hz), 120.1, 118.7, 118.6, 17.4; ESI-HRMS: *m/z* calculated for $C_{21}H_{15}BrF_3N_3NaO_2$: 500.0193; found 500.0193 [M + Na]$^+$.

5.1.4. (4-bromo-N-(2-methyl-5-(3-(trifluoromethyl)benzamido)phenyl) picolinamide)

To a solution of 4-bromopicolinic acid (1.1 g, 5.5 mmol) in THF (5 mL) and DCM (5 mL) and DMF (1.0 mL) was added oxalic chloride (0.47 mL, 5.5 mmol). The resulting solution was stirred for 2 h at rt. After concentration in vacuo, the residue was taken up in DCM (10 mL) and a solution of compound **2** (1.5 g, 5.0 mmol) and TEA (1.5 mL, 11 mmol) in DCM (10 mL) was added. The resulting mixture was stirred overnight and diluted with DCM (50 mL) and 1 M HCl (50 mL). The solids were collected by filtration, rinsed with water and DCM to obtain the product as a white solid (1.9 g, 79%). ^{1}H NMR (400 MHz, DMSO-d_6): δ = 10.52 (s, 1H), 10.29 (s, 1H), 8.74 (d, 1H, J = 5.3 Hz), 8.27 (m, 3H), 8.17 (d, 1H, J = 2.1 Hz), 7.96 (d, 1H, J = 7.8 Hz), 7.86 (dd, 1H, J = 2.1, 5.3 Hz), 7.80 (t, 1H, J = 7.8 Hz), 7.62 (dd, 1H, J = 2.2, 8.2 Hz), 7.27 (d, 1H, J = 8.4 Hz), 2.29 (s, 3H) ^{13}C NMR (101 MHz, DMSO-d_6): δ = 163.8, 160.9, 151.4, 150.2, 145.0, 137.0, 135.7, 135.6, 131.9, 130.2, 129.7, 129.1 (q, J = 32.0 Hz), 128.1 (q, J = 3.7 Hz), 126.9, 126.3, 124.0 (q, J = 272.6 Hz), 124.2 (q, J = 3.8 Hz), 122.3, 117.7, 115.8, 17.0; ESI-HRMS: *m/z* calculated for $C_{21}H_{15}BrF_3N_3NaO_2$: 500.0193; found 500.0201 [M + Na]$^+$.

5.1.5. (5-(1-methyl-1H-pyrazol-4-yl)-N-(2-methyl-5-(3-(trifluoromethyl) benzamido)phenyl)nicotinamide)

A solution of compound **3** (96 mg, 0.20 mmol), 1-methylpyrazole-4-boronic acid pinacol ester (42 mg, 0.20 mmol), Pd(PPh$_3$)$_4$ (23 mg, 20 μmol) and CsF (50 mg, 0.33 mmol) in MeOH/DMF (1:1, 2 mL) was reacted for 16 h at 70 °C. After concentration in vacuo and flash column chromatography (hexanes/EA 1:3 -> 0:1) the product was obtained as a white solid (65 mg, 68%). ^{1}H NMR (500 MHz, CDCl$_3$): δ = 9.29 (s, 1H), 8.90 (m, 2H), 8.67 (s, 1H), 8.17 (s, 1H), 8.05 (s, 1H), 7.94 (d, 1H, J = 7.8 Hz), 7.81 (s, 1H), 7.72 (s, 1H), 7.64 (m, 2H), 7.42 (t, 1H, J = 7.8 Hz), 7.24 (d, 1H, J = 8.3 Hz), 6.90 (d, 1H, J = 8.4 Hz), 3.85 (s, 3H), 1.93 (s, 3H); ^{13}C NMR (101 MHz, DMSO-d_6): δ = 164.4, 164.3, 149.0, 146.4, 137.3, 137.0, 136.4, 136.2, 132.3, 131.4, 130.8, 130.7, 130.2, 129.8, 129.5, 129.1, 128.8, 128.5 (q, J = 3.8 Hz), 124.7 (q, J = 3.8 Hz), 124.4 (q, J = 272.4 Hz), 119.2, 119.0, 118.4, 39.2, 17.9; ESI-HRMS: *m/z* calculated for $C_{25}H_{20}F_3N_5NaO_2$: 502.1467; found 502.1461 [M + Na]$^+$.

5.1.6. (2-(1-methyl-1H-pyrazol-4-yl)-N-(2-methyl-5-(3-(trifluoromethyl) benzamido)phenyl)isonicotinamide)

A solution of compound **4** (96 mg, 0.20 mmol), 1-methylpyrazole-4-boronic acid pinacol ester (42 mg, 0.20 mmol), Pd(PPh$_3$)$_4$ (23 mg, 20 μmol) and CsF (50 mg, 0.33 mmol) in THF/DMF (1:1, 3 mL) was reacted for 16 h at 70 °C. After concentration in vacuo and flash column chromatography (2% MeOH in EA) the product was obtained as a white solid (85 mg, 88%). ^{1}H NMR (400 MHz, DMSO-d_6): δ = 10.49 (s, 1H), 10.19 (s, 1H), 8.68 (d, 1H, J = 5.1 Hz), 8.35 (s, 1H), 8.29 (m, 2H), 8.10 (s, 1H), 8.05 (s, 1H), 7.96 (d, 1H, J = 7.8 Hz), 7.87 (s, 1H), 7.77 (t, 1H, J = 7.8 Hz), 7.62 (m, 2H), 7.29 (d, 1H, J = 8.2 Hz), 3.89 (s, 3H), 2.23 (s, 3H); ^{13}C NMR (101 MHz, DMSO-d_6): δ = 164.0, 163.9, 152.5, 150.1, 142.4, 137.2, 136.9, 135.8, 135.7, 131.9, 130.4, 129.9, 129.7, 129.4, 129.2 (q, J = 32.1 Hz), 128.2, 128.1, 124.2 (q, J = 3.8 Hz), 124.0 (q, J = 272.4 Hz), 122.4, 118.7, 118.6, 117.0, 25.1, 17.4; ESI-HRMS: *m/z* calculated for $C_{25}H_{20}F_3N_5NaO_2$: 502.1467; found 502.1461 [M + Na]$^+$.

5.1.7. (1-(2-fluoroethyl)-4-(4,4,5,5-tetramethyl-1,3,2-dioxaborolan-2-yl)-1H-pyrazole)

A suspension of 4-pyrazoleboronic acid pinacol ester (0.97 g, 5.0 mmol) and NaH (0.18 g, 7.5 mmol) in DMF (20 mL) was stirred for 30 min prior to the addition of 1-fluoro-2-iodoethane (0.45 mL, 5.5 mmol) and the resulting mixture was stirred overnight at rt. The mixture was diluted with Et$_2$O (100 mL) and washed with sat. NaHCO$_3$ (3 × 50 mL), 1 M HCl (3 × 50 mL) and brine (1 × 50 mL). The organic fraction was dried on Na$_2$SO$_4$, filtrated and concentrated in vacuo. Flash column chromatography (hexanes/EA 1:1) afforded the product as a colorless oil (0.35 g, 14%). ^{1}H NMR (400 MHz, CDCl$_3$): δ = 7.89 (s, 1H), 7.78 (m, 1H), 4.30 (t, 1H, J = 5.3 Hz), 3.85 (t, 1H, J = 5.4 Hz), 3.63 (t, 1H, J = 6.7 Hz), 3.16 (t, 1H, J = 6.7 Hz), 1.32 (d, 12H, J = 5.3 Hz); ^{13}C NMR (101 MHz, CDCl$_3$): δ = 145.8, 140.7, 137.5, 83.5 (d, J = 10.3 Hz), 70.7 (d, J = 260.1 Hz), 50.3, 24.9; ESI-HRMS: *m/z* calculated for $C_{11}H_{18}BFN_2NaO_2$: 263.1343; found: 263.1341 [M + Na]$^+$.

5.1.8. (5-(1-(2-fluoroethyl)-1H-pyrazol-4-yl)-N-(2-methyl-5-(3-(trifluoromethyl)benzamido)phenyl)nicotinamide)

A mixture of compound **3** (95 mg, 0.20 mmol), compound **7** (42 mg, 0.20 mmol), Pd(PPh$_3$)$_4$ (23 mg, 20 μmol) and CsF (50 mg, 0.33 mmol) in MeOH/THF (1:1, 3 mL) was refluxed for 16 h. After concentration in vacuo and flash column chromatography (EA/hexanes 3:1), the product was obtained as a yellow solid (75 mg, 73%). ^{1}H NMR (400 MHz, DMSO-d_6): δ = 10.51 (s, 1H), 10.17 (s, 1H), 9.06 (s, 1H), 8.96 (s, 1H), 8.50 (m, 2H), 8.32 (m, 2H), 8.16 (s, 1H), 7.95 (m, 2H), 7.79 (t, 1H, J = 7.8 Hz), 7.64 (d, 1H, J = 8.2 Hz), 7.31 (d, 1H, J = 8.2 Hz), 4.82 (dt, 2H, J = 47.3, 4.7 Hz), 4.50 (dt, 2H, J = 27.8, 4.7 Hz), 2.26 (s, 3H); ^{13}C NMR (101 MHz, DMSO-d_6): δ = 164.4, 164.3, 149.0, 146.6, 137.5, 137.3, 136.4, 136.2, 132.3, 131.9, 131.5, 130.8, 130.7, 130.2, 129.8, 129.6 (q, J = 32.8 Hz), 129.1, 128.7, 128.6 (q, J = 3.8 Hz), 124.7 (q, J = 3.8 Hz), 124.4 (q, J = 272.4 Hz), 119.2, 119.0, 118.5, 81.9 (d, J = 168.8 Hz), 52.6 (d, J = 19.9 Hz); ESI-HRMS: *m/z* calculated for $C_{26}H_{21}F_4N_5NaO_2$: 534.1529; found 534.1524 [M + Na]$^+$.

5.1.9. (N3-methyl-N5-(2-methyl-5-(3-(trifluoromethyl)benzamido) phenyl)pyridine-3,5-dicarboxamide)

To a solution of compound **3** (95 mg, 0.20 mmol), Pd(OAc)$_2$ (2.2 mg, 25 μmol), xantphos (12 mg, 50 μmol), NaOAc (41 mg, 0.50 mmol) in dioxane (4 mL) was added a solution of 2,4,6-trichlorophenyl formate (77 mg, 0.30 mmol) in toluene (1 mL). The resulting solution was heated at 80 °C in a closed vial for 16 h. After dilution with EA (10 mL) the mixture was filtered. The filtrate was concentrated in vacuo and resuspended in DMF (5 mL). Subsequently, TEA (0.28 mL, 2.0 mmol) and methylamine·HCl (0.13 g, 2.0 mmol) were added and the mixture was reacted for 3 h at rt. After dilution with EA (50 mL), the organic fraction was washed with 1 M HCl (50 mL) and brine (50 mL). After drying on Na$_2$SO$_4$, filtration and concentration, the product was purified using flash column chromatography (2% MeOH in EtOAc) to yield the product as a white solid (32 mg, 35%). ^{1}H NMR (400 MHz, DMSO-d_6): δ = 10.50 (s, 1H), 10.29 (s, 1H), 9.24 (s, 1H), 9.16 (s, 1H), 8.84 (d, 1H, J = 4.7 Hz), 8.71 (s, 1H), 8.30 (m, 2H), 7.98 (d, 1H, J = 7.8 Hz), 7.88 (s, 1H), 7.79 (t, 1H, J = 7.8 Hz), 7.61 (d, 1H, J = 8.4 Hz), 7.30 (d, 1H, J = 8.2 Hz), 2.85 (d, 3H, J = 4.3 Hz), 2.24 (s, 3H); ^{13}C NMR (101 MHz, DMSO-d_6): δ = 164.6, 163.9, 163.5, 150.6, 136.9, 135.9, 135.7, 134.3, 131.9, 130.4, 129.9, 129.8, 129.7, 129.3, 129.0, 128.2, 128.1, 124.2 (q, J = 3.8 Hz), 124.0 (q, J = 272.4 Hz), 118.7, 118.6, 26.3, 17.5; ESI-HRMS: *m/z* calculated for $C_{23}H_{19}F_3N_4NaO_3$: 479.1307; found: 479.1303 [M + Na]$^+$.

5.1.10. (N-(2-methyl-5-(3-(trifluoromethyl)benzamido)phenyl)-5-((trimethylsilyl)ethynyl)nicotinamide)

A mixture of compound **3** (0.48 g, 1.0 mmol), $PdCl_2(PPh_3)_2$ (70 mg, 0.10 mmol), CuI (19 mg, 0.10 mmol), TEA (0.6 mL, 4.0 mmol), and trimethylsilylacetylene (0.6 mL, 4.0 mmol) in DMF (5 mL) were stirred at rt for 16 h. After concentration in vacuo and purification by flash column chromatography (EA/hexanes 1:2) the product was obtained as a yellow solid (0.35 g, 71%). ^{1}H NMR (400 MHz, $CDCl_3$): $\delta = 8.95$ (m, 2H), 8.75 (s, 1H), 8.44 (s, 1H), 8.18 (s, 1H), 8.05 (s, 1H), 7.95, (d, 1H, $J = 7.8$ Hz), 7.82 (s, 1H), 7.70 (d, 1H, $J = 7.6$ Hz), 7.49 (t, 1H, $J = 7.7$ Hz), 7.24 (d, $J = 8.0$ Hz), 6.97 (d, $J = 8.1$ Hz), 2.00 (s, 3H), 0.27 (s, 9H); ^{13}C NMR (101 MHz, $CDCl_3$): $\delta = 164.9$, 164.2, 155.0, 147.1, 138.3, 136.3, 135.5, 134.9, 131.1 (q, $J = 32.7$), 130.9, 130.9, 129.7, 129.2, 128.5, 128.3 (q, $J = 3.6$ Hz), 124.5 (q, $J = 3.8$ Hz), 123.3 (q, $J = 272.5$ Hz), 120.8, 119.7, 118.2, 100.3, 100.3, 17.3, −0.2; ESI-HRMS: *m/z* calculated for $C_{26}H_{24}F_3N_3NaO_2Si$: 518.1488; found 518.1481 $[M + Na]^+$.

5.1.11. (5-ethynyl-N-(2-methyl-5-(3-(trifluoromethyl)benzamido)phenyl) nicotinamide)

To a solution of compound **10** (0.10 g, 0.20 mmol) in THF (2 mL) was added CsF (46 mg, 0.30 mmol) and the resulting solution was stirred overnight at room temperature. After filtration and concentration in vacuo, the product was purified by flash column chromatography (hexanes/EA 1:1 -> 1:2) yielding the product as a white solid (85 mg, quant.). ^{1}H NMR (400 MHz, CD_3OD): $\delta = 9.09$ (s, 1H), 8.82 (s, 1H), 8.43 (s, 1H), 8.25 (s, 1H), 8.20 (d, 1H, $J = 8.2$ Hz), 7.89 (d, 1H, $J = 7.8$ Hz), 7.83 (s, 1H), 7.74 (t, 1H, $J = 7.8$ Hz), 7.58 (dd, 1H, $J = 2.0$, 8.2 Hz), 7.31 (d, 1H, $J = 8.3$ Hz), 3.93 (s, 1H), 2.29 (s, 3H); ^{13}C NMR (101 MHz, CD_3OD): δ 167.0, 165.9, 155.5, 148.9, 139.8, 138.1, 137.3, 136.7, 132.3, 132.3, 132.0 (q, $J = 32.5$ Hz), 131.9, 131.6, 130.6, 129.3 (q, $J = 3.5$ Hz), 126.0 (q, $J = 271.7$ Hz), 125.6 (q, $J = 3.9$ Jz), 121.3, 121.0, 120.5, 83.9, 80.1, 17.7; ESI-HRMS: *m/z* calculated for $C_{23}H_{16}F_3N_3NaO_2$: 446.1092; found 446.1087 $[M + Na]^+$.

5.1.12. (5-(1-(2-fluoroethyl)-1H-1,2,3-triazol-4-yl)-N-(2-methyl-5-(3-(trifluoromethyl)benzamido)phenyl)nicotinamide)

To a 0.5 M solution of 1-azido-2-fluoroethane in DMF (0.30 mL, 0.15 mmol) was added **13** (30 mg, 71 μmol). Both a solution of sodium ascorbate (0.10 g, 0.51 mmol) in water (0.1 mL) and $CuSO_4{\cdot}5H_2O$ (12 mg, 50 μmol) in water (0.1 mL) were added and the mixture was reacted for 10 min at 80 °C using microwave irradiation. The resulting mixture was diluted with ethanol, filtered and purified by flash column chromatography (EA) to obtain the product as a white solid (20 mg, 55%). ^{1}H NMR (400 MHz, DMSO-d_6): $\delta = 10.49$ (s, 1H), 10.26 (s, 1H), 9.25 (d, 1H, $J = 2.0$ Hz), 9.09 (d, 1H, $J = 1.9$ Hz), 8.86 (s, 1H), 8.76 (t, 1H, $J = 2.1$ Hz), 8.29 (m, 2H), 7.96 (d, 1H, $J = 7.8$), 7.88 (d, 1H, $J = 2.1$ Hz), 7.79 (t, 1H, $J = 7.8$ Hz), 7.62 (dd, 1H, $J = 2.2$, 8.2 Hz), 7.29 (d, 1H, $J = 8.5$ Hz), 4.94 (m, 1H), 4.82 (m, 3H), 2.24 (s, 3H); ^{13}C NMR (101 MHz, DMSO-d_6): $\delta = 163.9$, 163.7, 148.7, 147.9, 143.1, 136.9, 135.9, 135.7, 131.9, 131.6, 130.4, 130.4, 129.7, 129.3, 129.2 (q, $J = 32.0$ Hz), 128.1 (q, $J = 3.8$ Hz), 126.4, 124.2 (q, $J = 3.9$ Hz), 124.0 (q, $J = 272.5$ Hz), 123.1, 118.7, 118.6, 81.9 (d, $J = 81.86$ Hz), 50.4 (d, $J = 19.5$ Hz), 17.5; ESI-HRMS: *m/z* calculated for $C_{25}H_{20}F_4N_6NaO_2$: 535.1482; found: 535.1476 $[M + Na]^+$.

*5.1.13. **(13)** (methyl 4-methyl-3-(trifluoromethyl)benzoate)*

To a mixture of 4-methyl-3-(trifluoromethyl)benzoic acid (2.04 g, 10.0 mmol) and K_2CO_3 (2.13 g, 15.0 mmol) in DMF (10 mL) was added methyl iodide (0.93 mL, 15 mmol) and the resulting mixture was stirred for 16 h at rt. After concentrating *in vacuo*, the residue was diluted with ethyl acetate (50 mL) and washed with subsequently H_2O (3 × 50 mL) and brine (50 mL). The organic fraction was dried on Na_2SO_4, filtered and concentrated in vacuo to obtain the title compound as a yellow oil (1.90 g, 87%). ^{1}H NMR (400 MHz, $CDCl_3$): $\delta = 8.27$ (s, 1H), 8.07 (d, 1H, $J = 7.9$ Hz), 7.36 (d, 1H, $J = 7.9$ Hz), 3.93 (s, 3H), 2.53 (s, 3H); ^{13}C NMR (101 MHz, $CDCl_3$): $\delta = 166.1$, 142.2 (q, $J = 1.6$ Hz), 132.7, 132.3, 129.4 (q, $J = 30.6$ Hz), 128.3, 127.3 (q, $J = 5.7$ Hz), 124.2 (q, $J = 273.8$ Hz), 52.5, 19.7.

5.1.14. (methyl 4-(bromomethyl)-3-(trifluoromethyl)benzoate)

To a solution of compound **13** (1.09 g, 5.00 mmol) and *N*-bromosuccinimide (1.78 g, 10.0 mmol) in acetonitrile (20 mL) was added benzoyl peroxide (0.12 g, 0.50 mmol) and the resulting solution was heated at reflux temperature for 16 h. After concentration *in vacuo*, the residue was taken up in ethyl acetate (50 mL) and washed with saturated $NaHCO_3$ (3 × 50 mL) and brine (50 mL). The organic fraction was dried on Na_2SO_4, filtered and concentrated *in vacuo*. After flash column chromatography (5% EA in hexanes) the product was obtained as a white solid (1.10 g, 74%). ^{1}H NMR (400 MHz, $CDCl_3$): $\delta = 8.32$ (d, 1H, $J = 1.5$ Hz), 8.20 (dd, 1H, $J = 1.7$, 8.1 Hz), 7.70 (d, 1H, $J = 8.1$ Hz), 4.64 (s, 2H), 3.96 (s, 3H); ^{13}C NMR (101 MHz, $CDCl_3$): $\delta = 165.4$, 140.9, 133.3, 133.1, 130.5, 128.7 (q, $J = 31.5$), 127.7 (q, $J = 5.6$ Hz), 123.7 (q, $J = 274.2$ Hz), 52.7, 27.5.

5.1.15. (methyl 4-((4-methylpiperazin-1-yl)methyl)-3-(trifluoromethyl) benzoate)

A mixture of compound **14** (0.89 g, 3.0 mmol), 1-methylpiperazine (0.90 g, 9.0 mmol) and K_2CO_3 (0.83 g, 6.0 mmol) in acetonitrile (20 mL) was heated at reflux temperature for 16 h, prior to concentration *in vacuo*. The residue was diluted with ethyl acetate (50 mL) and washed with saturated $NaHCO_3$ (3 × 50 mL). The organic fraction was concentrated *in vacuo* and the residue purified by flash column chromatography (5% MeOH in DCM) to obtain the product as a yellow solid (0.60 g, 63%). ^{1}H NMR (400 MHz, $CDCl_3$): $\delta = 8.28$ (d, 1H, $J = 1.4$ Hz), 8.16 (dd, 1H, $J = 1.5$, 8.1 Hz), 7.92 (d, 1H, $J = 8.2$ Hz), 3.93 (s, 3H), 3.69 (s, 2H), 2.51 (m, 8H), 2.29 (s, 3H); ^{13}C NMR (101 MHz, $CDCl_3$): $\delta = 166.0$, 143.4, 132.8, 130.6, 129.0, 129.0 (q, $J = 31.0$ Hz), 127.3 (q, $J = 6.2$ Hz), 124.1 (q, $J = 274.0$ Hz), 58.1, 55.3, 53.3, 52.5, 46.1; ESI-HRMS: *m/z* calculated for $C_{15}H_{20}F_3N_2O_2$: 317.1471; found: 317.1473 $[M + H]^+$.

5.1.16. (4-((4-methylpiperazin-1-yl)methyl)-3-(trifluoromethyl)benzoic acid

To a solution of compound **15** (0.47 g, 1.5 mmol) in ethanol (2 mL) was added 2 M NaOH (2 mL). The solution was stirred at rt for 6 h, prior to concentration in vacuo to approximately 2 mL. The solution was diluted to 10 mL with H_2O and the pH was adjusted to pH 5 using 1 M HCl. The aqueous phase was extracted with *t*BuOH (5 × 10 mL) and the combined organic fractions were dried on Na_2SO_4, filtered and concentrated to yield a white solid (0.21 g, 46%) that was used in the subsequent reaction without any further purification. ESI-HRMS: *m/z* calculated for $C_{14}H_{18}F_3N_2O_2$: 303.1315; found: 303.1315 $[M + H]^+$.

5.1.17. (5-bromo-N-(2-methyl-5-nitrophenyl)nicotinamide)

A solution of 2-methyl-5-nitroaniline (1.52 g, 10.0 mmol), 5-bromonicotinic acid (2.02 g, 10.0 mmol), EDC (2.11 g, 11.0 mmol) and DMAP (1.83 g, 15.0 mmol) in DMF (20 mL) was stirred at rt for 16 h. After concentrating in vacuo the residue was purified by flash column chromatography (DCM – 10% MeOH in DCM) to obtain the product as a white solid (2.00 g, 59%). ^{1}H NMR (400 MHz, DMSO-d_6): $\delta = 10.40$ (s, 1H), 9.10 (d, 1H, $J = 1.7$ Hz), 8.94 (d, 1H, $J = 2.0$ Hz), 8.57 (s, 1H), 8.38 (d, 1H, $J = 2.1$ Hz), 8.06 (dd, 1H, $J = 2.2$, 8.4 Hz), 7.59 (d, 1H, $J = 8.4$ Hz), 2.41 (s, 3H); ^{13}C NMR (101 MHz, DMSO-d_6): $\delta = 163.1$, 153.0, 147.5, 145.7, 141.6, 138.0, 136.7, 131.6, 131.4, 120.7, 120.6, 120.0, 18.2; ESI-HRMS: *m/z* calculated for $C_{13}H_{10}BrN_3NaO_3$: 357.9803; found: 357.9799 $[M + Na]^+$.

5.1.18. (5-(1-methyl-1H-pyrazol-4-yl)-N-(2-methyl-5-nitrophenyl) nicotinamide

A mixture of compound **17** (0.67 g, 2.0 mmol), 1-methylpyrazole-4-boronic acid pinacol ester (0.42 g, 2.0 mmol), $Pd(PPh_3)_4$ (58 mg, 50 μmol) and CsF (0.60 g, 4.0 mmol) in DMF (10 mL) was heated at 100 °C

for 16 h. The mixture was concentrated in vacuo, diluted with DCM (50 mL) and washed with saturated $NaHCO_3$ (3 × 50 mL) and brine (50 mL). The organic fraction was concentrated in vacuo and purified using flash column chromatography (gradient: DCM – 3% MeOH in DCM) to obtain the product as a yellow solid (0.20 g, 59%). %). ^{1}H NMR (400 MHz, DMSO-d_6): $\delta = 10.34$ (s, 1H), 9.04 (d, 1H, $J = 2.1$ Hz), 8.94 (d, 1H, $J = 2.0$ Hz), 8.46 (m, 1H), 8.40 (d, 1H, $J = 2.4$ Hz), 8.37 (s, 1H), 8.06 (m, 2H), 7.61 (d, 1H, $J = 8.5$ Hz), 3.91 (s, 3H), 2.43 (s, 3H); ^{13}C NMR (101 MHz, DMSO-d_6): $\delta = 164.5, 148.7, 146.0, 145.7, 141.6, 137.0, 136.5, 131.6, 131.2, 130.0, 129.7, 128.4, 120.6, 120.5, 117.8, 18.3$; ESI-HRMS: *m/z* calculated for $C_{17}H_{16}N_5O_3$: 338.1248; found: 338.1251 $[M + H]^+$.

5.1.19. (N-(5-amino-2-methylphenyl)-5-(1-methyl-1H-pyrazol-4-yl) nicotinamide

A mixture of compound **18** (0.10 g, 0.30 mmol), NH_4Cl (80 mg, 1.5 mmol), iron powder (84 mg, 1.5 mmol) in EtOH/H_2O (7:3, v/v, 5 mL) was heated at 70 °C for 2 h. The mixture was filtered over celite and dried in vacuo. The residue was diluted with DCM (25 mL) and washed with brine (25 mL). The organic fraction was dried on Na_2SO_4, filtered and concentrated in vacuo to obtain the product as a yellow solid (83 mg, 90%). ^{1}H NMR (400 MHz, DMSO-d_6): $\delta = 9.84$ (s, 1H), 8.99 (d, 1H, $J = 2.1$ Hz), 8.89 (s, 1H), 8.41 (s, 1H), 8.35 (s, 1H), 8.05 (s, 1H), 6.92 (d, 1H, $J = 8.3$ Hz), 6.61 (d, 1H, $J = 2.1$ Hz), 6.43 (dd, 1H, $J = 2.5, 8.2$ Hz), 4.94 (s, 2H), 3.90 (s, 3H), 2.07 (s, 3H); ^{13}C NMR (101 MHz, DMSO-d_6): $\delta = 163.9, 148.5, 146.1, 146.4, 136.7, 136.2, 131.1, 130.7, 130.6, 128.9, 128.5, 120.7, 118.1, 112.7, 112.5, 37.3, 17.1$; ESI-HRMS: *m/z* calculated for $C_{17}H_{18}N_5O$ 308.1506; found: 308.1508 $[M + H]^+$.

5.1.20. 5-(1-methyl-1H-pyrazol-4-yl)-N-(2-methyl-5-(4-((4-methylpiperazin-1-yl)methyl)-3-(trifluoromethyl)benzamido)phenyl) nicotinamide

To a solution of compound **16** (30 mg, 0.10 mmol), compound **19** (31 mg, 0.10 mmol), DMAP (37 mg, 0.30 mmol) in DMF (1 mL) was added EDC (29 mg, 0.15 mmol). The resulting solution was stirred for 16 h at rt. After concentration in vacuo the mixture was purified using flash column chromatography (5% MeOH in DCM) to obtain the product as a white solid (42 mg, 71%). ^{1}H NMR (400 MHz, DMSO-d_6): $\delta = 8.96$ (m, 2H), 8.54 (s, 1H), 8.25 (s, 1H), 8.20 (s, 1H), 8.16 (d, 1H, $J = 8.1$ Hz), 8.01 (s, 1H), 7.98 (d, 1H, $J = 8.2$ Hz), 7.85 (d, 1H, $J = 1.9$ Hz), 7.57 (dd, $J = 2.1, 8.3$ Hz), 7.32 (d, 1H, $J = 8.5$ Hz), 3.97 (s, 3H), 3.76 (s, 2H), 2.58 (bs, 8H), 2.35 (s, 3H), 2.32 (s, 3H); ESI-HRMS: *m/z* calculated for $C_{31}H_{33}F_3N_7O_2$: 592.2642; found: 592.2648 $[M + H]^+$.

5.2. In vitro IC_{50} determination

Affinities for designed compounds were determined using a commercially available Z'-LYTE™ assay according to the manufacturer's instructions. Briefly, in a 384 well plate were added the respective kinase (either CSF-1R, PDGFR-β or c-KIT in a final concentration of 0.5, 1.0 and 1.0 ng/μL, respectively) in supplied kinase buffer, ATP (in a final concentration of 50 μM for CSF-1R and PDGFR-β, 100 μM for c-KIT), the respective inhibitor (2-fold dilution series in a concentration range from 1 μM to 0.5 nM), and the assay FRET-peptide. The resulting solutions (total volume of 10 μL per well) were incubated at rt for 1 h, followed by the addition of protease solution (5 μL per well). After careful mixing, the solutions were incubated for 1 h followed by the addition of stop buffer (5 μL per well). Readout of the plate was performed using excitation wavelength of 400 nm and an excitation wavelength of 445 (coumarin) and 520 nm (fluorescein) with a 12 nm bandwidth. Negative control and positive control reactions were performed by omission of ATP and inhibitor, respectively. The obtained values are the result of three independent experiments and are expressed as average IC_{50} value ± standard deviation.

5.3. Radiosynthesis

$[^{11}C]CO_2$ was produced by the $^{14}N(p,\alpha)^{11}C$ nuclear reaction performed in a 0.5% O_2/N_2 gas mixture using an IBA Cyclone 18/9 cyclotron (IBA, Louvain-la-Neuve, Belgium). Radioactivity levels were measured using a Veenstra (Joure, The Netherlands) VDC-405 dose calibrator. After irradiation, $[^{11}C]CO_2$ was concentrated on a silica trap (−196 °C, 50 mg silica gel, 100/80 mesh). When the activity reached a maximum, the trap was heated and $[^{11}C]CO_2$ was passed over a gas purifier column (400 × 4 mm, silica gel, 100/80 mesh) using helium (30 mL·min^{-1}) as carrier gas. The purified $[^{11}C]CO_2$ was passed over a molybdenum reductor column heated at 850 °C (Sigma Aldrich, < 150 μm, 99.99%) after which unreacted $[^{11}C]CO_2$ was trapped on an ascarite column and $[^{11}C]CO$ was collected on a cooled silica trap (−150 °C, 1 mg silica gel, 100/80 mesh). The transfer gas was switched from helium to xenon (Fluka, ≥ 99.995). $[^{11}C]CO$ was released by heating of the trap and transferred by a gentle xenon flow (2.0 mL · min^{-1}) [20] to the previously charged and sealed reagent vial. For reaction optimization, $[^{11}C]CO$ was transferred to a collection syringe mounted on a automated syringe pump and subsequently dispensed over up to ten reaction vials [19], whereas for production runs the full batch of $[^{11}C]CO$ was transferred to a single reaction vial. For production runs, the vial was charged with a mixture of precursor **19** (3.0 mg, 10 μmol), trifluoro-iodobenzene (2.7 mg, 10 μmol), $PdCl_2(PPh_3)_2$ (1.4 mg, 2.0 μmol), xantphos (2.9 mg, 5.0 μmol), DMAP (3.0 mg, 20 μmol) in THF (0.7 mL). After transfer of $[^{11}C]CO$ to this reaction vial the reaction solution was heated at 100 °C for 5 min. Radioactivity levels in the reaction vial were measured after heating and after degassing of the reaction solution to determine trapping efficiency of $[^{11}C]CO$. A sample was taken for HPLC analysis to determine radiochemical purity. The reaction mixture was diluted with 1 mL of mobile phase and $[^{11}C]$**5** was isolated by preparative HPLC. Formulation for injection was performed by diluting the HPLC product fraction with H_2O (40 mL) and passing over a Seppak C18 light solid phase extraction cartridge (Waters, Milford, MA, USA). The cartridge was then washed with 10 mL of water followed by elution of the product from the cartridge with 1 mL of ethanol. The ethanol fraction was concentrated to 0.2 mL in vacuo at 80 °C with a helium flow of 50 mL·min^{-1} and diluted with 1.8 mL of saline to obtain a final concentration of 10% ethanol in saline. The identity of $[^{11}C]$**5** was confirmed by analytical HPLC by co-injection of both labeled and unlabeled compounds.

5.4. Partition coefficient LogD

The partitioning of $[^{11}C]$**5** between 1-octanol and 0.2 M phosphate buffer (pH = 7.4) was determined by vigorously mixing $[^{11}C]$**5** (100 μL, 10 MBq) with a solution of 0.2 M phosphate buffer (2 mL, pH 7.4) and 1-octanol (2 mL) for 1 min using a vortex apparatus. After a settling period of 1 h, three samples of 100 μL were taken from both layers. Samples were counted for radioactivity and the Log D values were calculated according to the following formula: Log $D_{oct,7.4}$ = Log ($A_{oct}/A_{phosphate\ buffer}$), where A_{oct} and $A_{phosphate}$ buffer represent average radioactivities of three 1-octanol and three phosphate buffer samples, respectively. The result is expressed as mean ± standard deviation (n = 3).

5.5. Radiometabolite analysis

Rats (14–16 weeks old, 250–300 g, n = 2) were injected with $[^{11}C]$**5** (250 μL, approximately 25 MBq) under isoflurane anesthesia (2% in O_2 at 1 L/min). After 1.5 h, animals were sacrificed and blood was collected by arterial puncture (approximately 0.5 mL) and transferred to a Heparin coated Eppendorf tube. In addition, the left hemisphere was collected. Blood samples were centrifuged for 5 min at 4600 RPM to separate blood plasma from cells. The plasma (100 μL) was diluted in acetonitrile (200 μL at 0 °C) and centrifuged for 5 min at 15,000 RPM for removal of proteins. Brains were homogenized in acetonitrile (200 μL at

0 °C) and centrifuged for 5 min at 15,000 RPM. An aliquot of each supernatant (10 μL) was transferred to a TLC plate, which was subsequently dried at room temperature for 5 min and ran in a solution of DCM/MeOH (90:10, v/v). The radioTLC plate was transferred to a phosphorimager storage screen and left for 1 h. Readout was performed on a Typhoon phosphorimager and subsequent analysis was performed using ImageQuant.

5.6. PET scanning

Dynamic PET imaging was performed using dedicated small animal NanoPET/CT and NanoPET/MR scanners (Mediso Ltd., Hungary, Budapest) with identical PET components. Rats (n = 2 per group) were anaesthetized with 4 and 2% isoflurane in 1 $L \cdot min^{-1}$ O_2 for induction and maintenance, respectively. Rats were positioned on the scanner bed, and the respiratory rate was monitored for the duration of the scan, adjusting anaesthesia when required. A dynamic PET scan was acquired immediately after intravenous (i.v.) administration (tail vein) of 25 MBq [^{11}C]**5**. For efflux blocking experiments, rats received tariquidar 30 min prior to tracer injection (15 $mg \cdot kg^{-1}$). Data was analyzed using VivoQuant, by drawing a region of interest around the full brain. Results are expressed as percentage injected dose per gram (%ID/g). Error bars indicate standard deviation.

5.7. In vitro autoradiography

Autoradiography was performed in flash frozen rat brain sections (10 μm thickness). Sections were washed with 50 mM Tris-HCl buffer (pH 7.4) for 15 min. After drying under a gentle air flow the section were incubated with [^{11}C]**5** (0.5 $MBq \cdot mL^{-1}$) in 50 mM Tris-HCl, pH 7.4 in the absence or presence of a CSF-1R inhibitor at 1 μM concentration for 30 min. Washing was performed with cold Tris-HCl (5 mM, 4 °C, two times) followed by dipping in ice cold water. After drying in an air stream, rat brain sections were exposed to a phosphorimaging screen (GE Healthcare, Buckinghamshire, UK) for 10 min and developed on a Typhoon FLA 7000 phosphor imager (GE Healthcare, Buckinghamshire, UK). Visualisation of binding was performed using ImageQuantTL v8.1.0.0 (GE Healthcare, Buckinghamshire, UK).

Funding

The project was supported, in part, by The Ben and Catherine Ivy Foundation (FTC), the National Cancer Institute: R21 CA205564 (FTC), the National Institutes of Health: S10 OD018130 (FTC) and the Dutch Research Council (BvdW, NWO-VENI grant (VI.Veni.192.229).

Declaration of Competing Interest

The authors declare that they have no known competing financial interests or personal relationships that could have appeared to influence the work reported in this paper.

Appendix A. Supplementary material

Supplementary data to this article can be found online at https://doi.org/10.1016/j.bmc.2021.116245.

References

1 Akiyama H, Nishimura T, Kondo H, et al. Expression of the receptor for macrophage colony stimulating factor by brain microglia and its upregulation in brains of patients with Alzheimer's disease and amyotrophic lateral sclerosis. *Brain Res*. 1994;639:171–174.
2 Chitu V, Gokhan Ş, Nandi S, Mehler MF, Stanley ER, et al. Emerging roles for CSF-1 receptor and its ligands in the nervous system. *Trends Neurosci*. 2016;39:378–393.
3 Li Q, Barres BA. Microglia and macrophages in brain homeostasis and disease. *Nat Rev Immunol*. 2018;18:225–242.
4 Pyonteck SM, Akkari L, Schuhmacher AJ, et al. CSF-1R inhibition alters macrophage polarization and blocks glioma progression. *Nat Med*. 2013;19:1264–1272.
5 Elmore MR, Najafi AR, Koike MA, et al. Colony-stimulating factor 1 receptor signaling is necessary for microglia viability, unmasking a microglia progenitor cell in the adult brain. *Neuron*. 2014;82:380–397.
6 Spangenberg E, Severson PL, Hohsfield LA, et al. Sustained microglial depletion with CSF1R inhibitor impairs parenchymal plaque development in an Alzheimer's disease model. *Nat Commun*. 2019;10:3758.
7 Peyraud F, Cousin S, Italiano A. CSF-1R inhibitor development: current clinical status. *Curr Oncol Rep*. 2017;19:70.
8 Bernard-Gauthier V, Schirrmacher R. 5-(4-((4-[(^{18})F]Fluorobenzyl)oxy)-3-methoxybenzyl)pyrimidine-2,4-diamine: A selective dual inhibitor for potential PET imaging of Trk/CSF-1R. *Bioorg Med Chem Lett*. 2014;24:4784–4790.
9 Tanzey SS, Shao X, Stauff J, et al. Synthesis and initial in vivo evaluation of [^{11}C] AZ683 - A novel PET radiotracer for colony stimulating factor 1 receptor (CSF1R). *Pharmaceuticals*. 2018;11:136.
10 Horti AG, Naik R, Foss CA, et al. PET imaging of microglia by targeting macrophage colony-stimulating factor 1 receptor (CSF1R). *PNAS*. 2019;116:1686–1691.
11 Illig CR, Chen J, Wall MJ, et al. Discovery of novel FMS kinase inhibitors as anti-inflammatory agents. *Bioorganic Med Chem Lett*. 2008;18:1642–1648.
12 Illig CR, Manthey CL, Wall MJ, et al. Optimization of a potent class of arylamide colony-stimulating factor-1 receptor inhibitors leading to anti-inflammatory clinical candidate 4-cyano-*N*-[2-(1-cyclohexen-1-yl)-4-[1-(dimethylamino)- acetyl]-4-piperidinyl]phenyl]-1H-imidazole-2-carboxamide (JNJ-28312141). *J Med Chem*. 2011;54:7860–7883.
13 Van der Wildt B, Miao Z, Park JH, et al. Carbon-11 labeled BLZ945 as PET tracer for Colony Stimulating Factor 1 Receptor imaging in the brain. *J Labelled Compd Radiopharm*. 2019;62:S487–S488.
14 Ramachandrana SA, Jadhavara PS, Miglania SK, et al. Design, synthesis and optimization of bis-amide derivatives as CSF1Rinhibitors. *Bioorg Med Chem Lett*. 2017;27:2153–2160.
15 Miyaura N, Yamada K, Suzuki A. A new stereospecific cross-coupling by the palladium-catalyzed reaction of 1-alkenylboranes with 1-alkenyl or 1-alkynyl halides. *Tet Lett*. 1979;20:3437–3440.
16 Ueda T, Konishi H, Manabe K. Trichlorophenyl formate: highly reactive and easily accessible crystalline CO surrogate for palladium-catalyzed carbonylation of aryl/alkenyl halides and triflates. *Org Lett*. 2012;14:5370–5373.
17 Sonogashira K. Development of Pd-Cu catalyzed cross-coupling of terminal acetylenes with sp2-carbon halides. *J Organomet Chem*. 2002;653:46–49.
18 Rostovtsev VV, Green LG, Fokin VV, et al. A stepwise Huisgen cycloaddition process: copper(I)-catalyzed regioselective "ligation" of azides and terminal alkynes. *Angew Chem Int Ed*. 2002;41:2596–2599.
19 Van der Wildt B, Shen B, Chin FT. A [^{11}C] CO dispensing system for rapid screening of carbonylation reactions. *J Label Compd Radiopharm*. 2018;61(14):1110–1114.
20 Eriksson J, Van den Hoek J, Windhorst AD. Transition metal mediated synthesis using [^{11}C]CO at low pressure—a simplified method for 11C-carbonylation. *J Label Compd Radiopharm*. 2012;55:223–228.
21 Dahl K, Schou M, Amini N, et al. Palladium-mediated [^{11}C]Carbonylation at atmospheric pressure: a general method using xantphos as supporting ligand. *Eur J Org Chem*. 2013:1228–1231.
22 Karimi F, Langström B. Synthesis of 11C-labelled amides by palladium-mediated carboxamination using [11C]carbon monoxide, in situ activated amines and 1,2,2,6,6-pentamethylpiperidine. *Eur J Org Chem*. 2003;11:2132–2137.
23 Van der Wildt B, Wilhelmus MMM, Bijkerk J, et al. Development of carbon-11 labeled acryl amides for selective PET imaging of active tissue transglutaminase. *Nuc Med Biol*. 2016;43(4):232–242.
24 Peng Z, Maxwell DS, Sun D, et al. Imatinib analogs as potential agents for PET imaging of Bcr-Abl and c-KIT expression at a kinase level. *Bioorg Med Chem*. 2014;22:623–632.
25 Kil KE, Ding YS, Lin KS, et al. Synthesis and positron emission tomography studies of carbon-11-labeled imatinib (Gleevec). *Nucl Med Biol*. 2007;34:153–163.
26 Cai H, Shi Q, Tang Y, et al. Positron emission tomography imaging of platelet-derived growth factor receptor β in colorectal tumor xenograft using zirconium-89 labeled dimeric affibody molecule. *Mol Pharmaceut*. 2019;16:1950–1957.
27 Tolmachev V, Varasteh Z, Honarvar H, et al. Imaging of platelet-derived growth factor receptor beta expression in glioblastoma xenografts using affibody molecule ^{111}In-DOTA-Z09591. *J Nucl Med*. 2014;55:294–300.
28 Slobbe P, Poot A, Windhorst AD, et al. PET imaging with small-molecule tyrosine kinase inhibitors: TKI-PET. *Drug Discovery Today*. 2012;17:1175–1187.
29 Wakabayashi Y, Telu S, Dick RM, et al. Discovery, radiolabeling, and evaluation of subtype-selective inhibitors for positron emission tomography imaging of brain phosphodiesterase-4D. *ACS Chem Neurosci*. 2020;11:1311–1323.
30 Mathews WB, Burns HD, Dannals RF, et al. Carbon-11 labeling of a potent, nonpeptide, at1-selective angiotensin-II receptor antagonist: MK-996. *J Labelled Compd Radiopharm*. 1995;36:729–737.
31 Van der Wildt B, Shen B, Chin FT. Efficient synthesis of carbon-11 labelled acylsulfonamides using [11C]CO carbonylation chemistry. *Chem Commun*. 2019;55:3124–3127.
32 Dahl K, Itsenko O, Rahman O, et al. An evaluation of a high-pressure ^{11}CO carbonylation apparatus. *J Label Compd Radiopharm*. 2020;58:220–225.
33 Van der Born D, Sewing C, Herscheid JDM, et al. A universal procedure for the [F-18] trifluoromethylation of aryl iodides and aryl boronic acids with highly improved specific activity. *Angewandte Chem-Int Ed*. 2014;53:11046–11050.
34 Bankstahl JP, Kuntner C, Abrahim A, et al. Tariquidar-induced P-glycoprotein inhibition at the rat bloodbrain barrier studied with (R)-^{11}C-verapamil and PET. *J Nucl Med*. 2008;49:1328–1335.

35 Bankstahl JP, Bankstahl M, Römermann K, et al. Tariquidar and elacridar are dose-dependently transported by P-glycoprotein and Bcrp at the blood-brain barrier: a small-animal positron emission tomography and in vitro study. *Drug Metab Dispos*. 2013;41:754–762.

36 Rankovic Z. CNS drug design: balancing physicochemical properties for optimal brain exposure. *J Med Chem*. 2015;58:2584–2608.

37 Wager TT, Hou X, Verhoest PR, et al. Moving beyond rules: the development of a central nervous system multiparameter optimization (CNS MPO) approach to enable alignment of druglike properties. *ACS Chem Neurosci*. 2010;1:435–439.